Enzyme-integrated cholesterol biosensing scaffold based on in situ synthesized reduced graphene oxide and dendritic Pd nanostructure

Ramendra Sundar Dey, C. Retna Raj

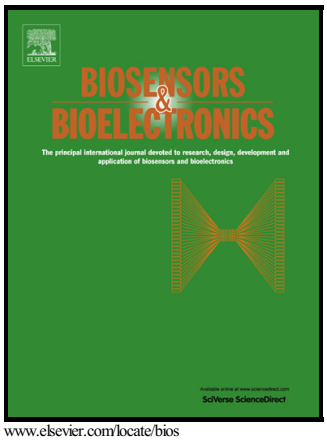

www.elsevier.com/locate/bios

PII: S0956-5663(14)00486-2
DOI: http://dx.doi.org/10.1016/j.bios.2014.06.063
Reference: BIOS6897

To appear in: *Biosensors and Bioelectronic*

Received date: 4 July 2014
Revised date: 4 July 2014
Accepted date: 4 July 2014

Cite this article as: Ramendra Sundar Dey and C. Retna Raj, Enzyme-integrated cholesterol biosensing scaffold based on in situ synthesized reduced graphene oxide and dendritic Pd nanostructure, *Biosensors and Bioelectronic,* http://dx.doi.org/10.1016/j.bios.2014.06.063

Enzyme-Integrated Cholesterol Biosensing Scaffold Based on In Situ Synthesized Reduced Graphene Oxide and Dendritic Pd Nanostructure

Ramendra Sundar Dey and C. Retna Raj*

Department of Chemistry, Indian Institute of Technology, Kharagpur 721302, India

*Corresponding author, E-mail: crraj@chem.iitkgp.ernet.in, Fax: 91-3222-282522

Graphical Abstract

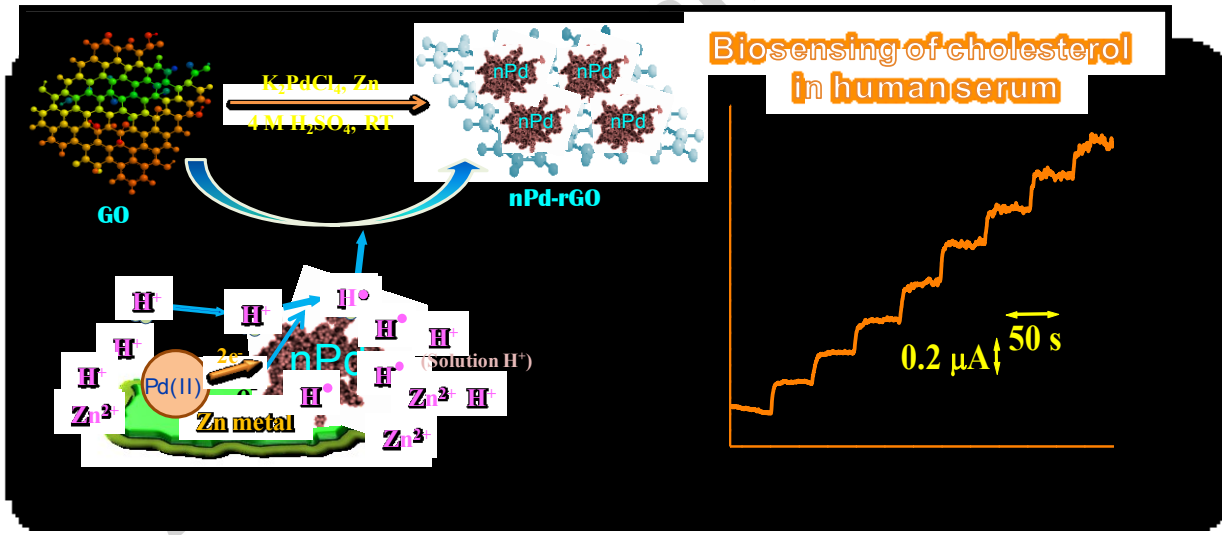

ABSTRACT

A new approach for the one-pot synthesis of reduced graphene oxide-dendritic Pd nanoparticle (rGO-nPd) hybrid material and the development of biosensing scaffold for the amperometric sensing of H_2O_2 and total cholesterol in human serum are described. In situ reduction of both graphene oxide (GO) and $PdCl_4^{2-}$ in acidic solution was achieved with Zn to yield rGO-nPd hybrid material. The oxygen containing functionalities of GO were reduced by the liberated atomic hydrogen in 20 min. The formal potential of Zn/Zn^{2+} and $PdCl_4^{2-}/Pd$ couples favor the facile reduction of $PdCl_4^{2-}$. The in situ produced Pd nanoparticles behave like hydrogen sponge and increase the local concentration of atomic hydrogen. Biosensing platform for H_2O_2 and cholesterol in human serum and butter sample was developed using the hybrid material. Amperometric sensing of H_2O_2 at 0.2 nM level without any redox mediator or enzymes in neutral pH is demonstrated. The cholesterol biosensing platform was developed by integrating cholesterol oxidase and cholesterol esterase with the hybrid material. The biosensor is highly sensitive (5.12 ± 0.05 $\mu A/\mu M cm^2$) and stable with a fast response time of 4s; it could detect cholesterol ester as low as 0.05 μM (S/N=3). The biosensor is successfully used for the analysis of total cholesterol in human serum and butter.

Keywords

Reduced Graphene oxide, Pd nanoparticle, Amperometric biosensor, H_2O_2, Cholesterol.

1. Introduction

The design and development of amperometric sensing and biosensing platforms for the quantification of bioanalytes such as H_2O_2, one of the reactive oxygen metabolites, in cellular environment and cholesterol, uric acid, etc. in biological fluids is of great interest in biology and biomedicine. H_2O_2 has dual role in the physiological system and it has been considered as a "*necessary evil*" (Rhee et al., 2006; Dröge et al., 2007; Sevanian et al., 1985). It involves in the normal function of cell signaling and it is a killing agent released from immune cell. However, its abnormal generation causes the oxidative stress and is associated with ageing, cancer and Parkinson's and Alzheimer's diseases (Li et al., 2011). The precise quantification of H_2O_2 in cellular environment is of broad interest for the diagnosis and monitoring of the diseases. On the other hand, cholesterol and its fatty acids esters are the primary constituents of all mammalian cells, and is also precursor for the biosynthesis of steroid hormones, vitamin D and bile acids (Myant et al., 1981). The undesired accumulation of cholesterol in serum leads to serious life threatening diseases like coronary heart diseases, cerebral thrombosis, myocardial infarction, hypertension and atherosclerosis. The normal concentration of total cholesterol in serum for a healthy person should be less than 200 mg/dL (<5.17 mM). The borderline high value of total cholesterol is defined as 200-239 mg/dL (5.17-6.18 mM) and the high value is above 240 mg/dL (≥6.21 mM) (Motonaka et al., 1993). The colorimetric methods have been traditionally used for the sensing of these bioanalytes. The poor sensitivity, selectivity and reliability of these conventional methods demand for alternative procedures or sensing devices for the quantification of the analytes without compromising the sensitivity and selectivity. The electrochemical methods are of great interest and received significant attention in the biosensor

and bioelectronic industries. The transducers based on metal nanoparticles are known to have enhanced sensitivity, selectivity and fast response time towards H_2O_2 and other metabolites (Safavi et al., 2007; Karam et al., 2008; Hrapovic et al., 2008; Yang et al., 2006; Lu et al., 2008). Among these, Pt and Pt-based alloys have been widely used in the past and good sensitivity and low detection limit have been achieved (Hrapovic et al., 2008; Yang et al., 2006; Lu et al., 2008). One of the major concerns with the Pt-based catalysts is that they require high detection potential (>0.4 V vs Ag/AgCl), which actually invites interference due to coexisting other easily oxidizable analytes. As the biological fluids such as serum contains high concentration of other analytes, protein, etc., it is desirable to develop a sensing platform which can be operated at low potential for the measurement of H_2O_2, cholesterol, etc. The nanostructured Pd with suitable shape and morphology can be an ideal choice due to its high catalytic activity, high abundance and relatively cheaper than Pt.

Synthesis of new multifunctional materials is of great interest in the development of biosensors and bioelectronic devices (Pumera et al., 2011; Wang et al., 2013; Lightcap et al.). The functional materials required for the development of such devices should have high electronic conductivity, mechanical strength, flexibility and good biocompatibility. The organic-inorganic hybrid materials derived from one atom thick graphene or reduced graphene oxide (rGO) and metal/metal oxide nanostructures are very promising for biosensing and bioelectronic applications, as they can provide ideal environment for the redox proteins and enzymes (Raj. 2013; Wang et al., 2013; Zan et al., 2013; Cui et al., 2013). The exceptional electronic conductivity, mechanical strength, biocompatibility, large accessible surface area and flexibility of rGO make it an excellent candidate in the development of biosensors (Raj et al., 2013; Wang

et al., 2013; Zan et al., 2013; Cui et al., 2013). The hybrid material of rGO and transition metal nanostructures is anticipated to show outstanding biosensing performance in terms of sensitivity, low detection limit, fast response time, etc. The metal nanostructures supported on the electronically conductive rGO sheets can efficiently catalyze the electrode reaction and hence high sensitivity and fast response time can be achieved (Zhu et al., 2010). The enhanced performance of the biosensors based on metal nanoparticles decorated rGO sheets has been recently documented in the literature (Tian et al., 2013; Artiles et al., 2011; Gutés et al., 2012).

Traditionally, the rGO-metal nanoparticle hybrid materials are synthesized by two-step approach involving the reduction of GO to rGO and metal precursors to corresponding zero valent metals followed by the mixing of both rGO and metal nanoparticles under optimized condition (Fang et al., 2010). One of the major disadvantages in the two-step approach is the re-stacking of the exfoliated individual rGO sheets. The hybrid materials have also been obtained by the reduction of metal precursors in the presence of rGO (Guo et al., 2010). Another interesting approach for the synthesis of rGO-metal nanoparticle is the in situ reduction of both GO and metal precursor in one-pot. The reducing agents capable of reducing both GO and metal precursors are critically required in this approach. The advantages of this approach is that the (i) unwanted restacking of rGO sheets can be avoided, (ii) uniform distribution of nanoparticles on the rGO sheets can be achieved and (iii) GO/rGO can function as a template for the growth of metal nanoparticles. The nature of reducing agent and the reaction conditions are known to play key role in controlling the reduction of oxygen functionalities of GO and regulating shape and morphology of the metal nanoparticles. The controlled reduction can yield anisotropic metal nanostructures. Various chemical methods with different reducing agents such as hydrazine,

sodium borohydride, ascorbic acid, metals, etc. have been used in the past for the reduction of GO (Guo et al., 2010; Yang et al., 2011; Jin et al., 2010; He et al., 2011; Barman et al., 2013; Prashant et al., 2010). Most of these methods are time consuming and involve toxic reducing agents and non eco-friendly solvents or hydrothermal conditions. The harsh reaction condition is known to introduce unwanted defects in the rGO sheets and severely alter the properties. Development of room temperature eco-friendly methods for the synthesis of rGO-metal nanoparticle hybrid materials for biosensing application is desired in order to retain the integrity of the individual components.

Herein we describe a new eco-friendly method for the synthesis of catalytically active hybrid material based on rGO and Pd nanoparticles (nPd) and the development of sensitive amperometric sensing platform for the low potential detection of H_2O_2 and cholesterol ester. The rGO-nPd hybrid material is able to sense H_2O_2 at the potential of ~0.25 V, which is significantly lower than the traditional Pt-based catalyst. The cholesterol biosensing platform was developed by integrating the enzymes with the hybrid material.

2. Material and methods

2.1. Reagents and materials

Graphite powder (<45 micron, >99.99%), H_2O_2 (30%), K_2PdCl_4, Nafion® (5 wt % solution in lower aliphatic alcohol containing 15-20% water), cholesterol, cholesteryl stearate, uric acid (UA), ascorbic acid (AA), ethanol (99.9%), ChOx (from *Streptomyces* sp., 54 units/mg), and ChEt (from *Pseudomonas fluorescens*, 13.16 units/mg) were obtained from Sigma-Aldrich and used as received. All other chemicals used in this investigation were of

analytical grade (99.9%). Phosphate buffer solution (PBS, 0.1 M) of pH 7.2 was used as supporting electrolyte for all voltammetric and amperometric measurements. All the solutions used in this investigation were prepared with Millipore water (Milli-Q system). Zn filings (≥ 99%) of average size ~0.5 cm with thickness of ~1 mm were used in this investigation.

2.2. Material Characterization

FTIR measurements were performed with Perkin Elmer FTIR spectrophotometer RX1. KBr pellet were used to prepare the samples for FTIR measurements. Raman measurements were carried out with a HORIBA JOBIN YVON (France, model no. T64000) equipped with a peltier-cooled CCD detector. The samples were excited with an air cooled argon ion laser of wavelength 514.5 nm with power 120 mW. XRD analysis was carried out with Panalytical high resolution X'pert PRO X-ray diffraction unit using Ni filtered CuKα (λ = 1.54 Å). Powder samples were directly used for the XRD measurements. XPS measurements were performed with PHI 5000 VersaProbe II scanning XPS microprobe (ULVAC-PHI, inc.) using the energy source Al (K_α, hν=1486.6 eV). The spectra were analyzed using casaXPS software. TEM measurements were performed with Analytical TEM (FEI-TECNAI G2 20S-TWIN) instruments operating at 200 kV. Energy-dispersive X-ray spectroscopic (EDX) measurement was carried out with FEI TECNAI-G2-20S-TWIN instruments with EDAX-EDS attachments (Model No. 942409761751, Standard-2). Carbon-coated copper grid (Pelco International, USA) was used for the sample preparation. All the voltammetric and amperometric measurements were carried out with CHI643B electrochemical analyzer attached to a Faraday cage/current booster (CH Instruments, Austin, TX). A two-compartment three-electrode cell with a glassy carbon electrode (GCE) working (0.07 cm^2), a platinum wire auxiliary and Ag/AgCl (3 M KCl) reference electrodes was used in

all the voltammetric and amperometric measurements. Miniaturized biosensor was performed with disposable screen printed electrode (SPEs, Dropsens, Spain) with small volume (50 μL) of electrolyte. The SPE is equipped with a carbon working (4 mm diameter), counter and silver reference electrodes. The SPEs were connected to the potentiostat using a DRP-DSC connector (Dropsens, Spain).

2.3. Synthesis of GO and rGO-nPd

GO was synthesized according to modified Hummer's method (Hummer et al., 1958; Kovtyukhova et al., 1999) by the exfoliation of graphite. Briefly, 50 mL concentrated H_2SO_4 was slowly added to a mixture of graphite powder (1 g) and $NaNO_3$ (1 g) in a 500 mL round bottom flask at 0 °C. Solid $KMnO_4$ (6 g) was added to the reaction mixture at <5 °C and the mixture was stirred continuously for 1 hr at room temperature. Water (200 mL) was slowly added to the mixture and the stirring was continued for another 15 min. Then 30% H_2O_2 solution was added to the reaction vessel until the gas evolution was ceased. The resulting mixture was centrifuged in an ultra centrifuge to remove the unexfoliated graphite and oxidizing agents. The residue was then washed repeatedly with 5% HCl solution until the washing solution give negative test for the presence of sulfate ions with $BaCl_2$ solution. The residue obtained after repeated washing was further washed with copious amount of Millipore water and dried in vacuum to get the yellow brown solid of GO.

The rGO-nPd hybrid material was synthesized by the *in situ* reduction of both GO and Pd(II) in acidic solution using Zn. Typically, first GO (10 mg) was dispersed in 4 M H_2SO_4 (10 mL) containing K_2PdCl_4 (1 mM) by ultrasonication for 30 min. Then, solid Zn fillings (1.0 g)

was slowly added to the reaction mixture and stirred vigorously for 20 min. During the addition of solid Zn fillings, the yellow brown color of the reaction mixture turned to black. The black colored rGO-nPd hybrid material was collected by centrifugation with an ultra centrifuge. The supernatant solution was colorless and it does not show any characteristic spectral band for the K_2PdCl_4, confirming the complete reduction of the precursor and adsorption of Pd nanoparticle on the surface of rGO. The rGO-nPd hybrid material was washed repeatedly with millipore water and dried at room temperature under vacuum. The amount of nPd in the hybrid material was 106 mg/g. The hybrid material with different loading of nPd was obtained by changing the concentration of K_2PdCl_4 with same amount of GO (1 mg/mL of water).

2.4. Fabrication of Biosensors

GCE or SPEs were used as a conducting substrate for the development of biosensing platform (Scheme S1). The GCE was first polished to mirror finish alumina slurry and washed repeatedly with Millipore water followed by sonication in water for 10 min. The rGO-nPd hybrid material (1 mg) was mixed with 1 % (v/v) of ethanolic Nafion® solution and sonicated for 5 min to get homogeneous dispersion. This suspension (5 µL) was drop casted on the cleaned GCE and dried at room temperature for 1 h. The dried electrode was subjected to electrochemical measurement and it was stored in PBS at 4 °C when not in use. For the biosensing of total cholesterol, the enzymes ChOx (10 mg) and ChEt (5 mg) were mixed with 10 µL 0.01 M PBS and stored at 4 °C. An aliquot of 5 µL of the enzyme mixture was drop casted on the rGO-nPd modified GCE and dried at 4 °C for 6 h. For the amperometric sensing of total cholesterol with SPEs, the working electrode of the screen printed strip was modified with rGO-nPd hybrid

material as in the case of GCE. The amperometric measurements using SPEs were performed with 50 μL of 0.1 M PBS as supporting electrolyte.

2.5. Sample preparation

The serum samples were collected from B. C. Roy Technology Hospital, IIT Kharagpur for the analysis of total cholesterol. The serum sample was diluted to 10 times with PBS to avoid the matrix effect and used directly for amperometric measurements. Cholesterol from commercially available butter sample was extracted according to the literature procedure (Peña et al., 2001). Briefly, 7.5 g of the butter sample was mixed with 20 mL of 1 M KOH and 10 mL of EtOAc. The resultant mixture was refluxed for 30 min under constant stirring. The insoluble residue was rejected after centrifugation in an ultra centrifuge and volume was adjusted to 50 mL by EtOAc. This solution was directly used in the amperometric measurements of total cholesterol in butter sample.

3. Results and discussion

3.1. Synthesis of rGO-nPd hybrid materials

The hybrid material was synthesized by one-pot approach at room temperature using Zn and mineral acid. Scheme 1 depicts the plausible mechanistic pathway for the reduction of GO and $PdCl_4^{2-}$ by metallic Zn in acid medium. Zn is capable of effectively reducing the oxygen containing functionalities of GO [Dey et al., 2012] at room temperature in 2 h (Figure S1) in the absence of $PdCl_4^{2-}$. However, in the presence of $PdCl_4^{2-}$, the reaction is highly facile and complete reduction of GO was achieved in 20 min. In the absence of Zn, $PdCl_4^{2-}$ could not

reduce GO, even after prolonged stirring, indicating the vital role of Zn in the reaction. The examination of the formal potential of Zn^{2+}/Zn (-0.763 V) and $PdCl_4^{2-}/Pd$ (+0.92 V) clearly indicates that Zn is thermodynamically capable of reducing $PdCl_4^{2-}$ to Pd instantaneously. It was observed from a control experiment (absence of GO) that Zn instantly reduces $PdCl_4^{2-}$ to Pd. Addition of Zn to the reaction mixture containing GO and $PdCl_4^{2-}$ in acidic solution, instantly reduces $PdCl_4^{2-}$ to Pd(0) and generate large amount of nascent hydrogen. It is well known that Pd is capable of absorbing hydrogen 900 times more than its volume (Weast et al., 1983-1984) and it can soaks up hydrogen like a sponge. The newly born nPd in the reaction mixture actually function as sponge for hydrogen and facilitates the reduction of oxygen containing functionalities of GO by increasing the local concentration of atomic hydrogen. As the presence of nPds essentially increases the local concentration of hydrogen, the complete reduction of GO was achieved in 20 min time. Moreover, it has been established earlier that the hydrogen intercalated Pd is a powerful reducing agent (Cheng et al., 1997). In the present case, either the in situ generated nascent hydrogen or the hydrogen intercalated Pd efficiently reduces the oxygen functionalities. The involvement of both routes cannot be ruled out.

3.2. Characterization of GO and rGO-nPd

To understand the progress of the reduction of GO, time-dependent FTIR spectral measurements were performed (Figure 1(a)). The spectra of GO shows the characteristic stretching frequencies for oxygen containing functional groups such as C=O (1720 cm^{-1}), O-H (3410 cm^{-1}), alkoxy C-O (1050 cm^{-1}), epoxy C-O (1227 cm^{-1}) and carboxylic C-O (1320-1210 cm^{-1}). Gradual decrease in the intensity of characteristic peaks corresponding to all oxygen functionalities was observed during the progress of the reaction. All the peaks for oxygen

functionalities completely disappeared within 20 min, confirming the reduction. It should be noted here that the reduction requires 2 h in the absence of $PdCl_4^{2-}$ (Figure S1 in the ESM). The new peak observed at 1548 cm^{-1} is attributed for the skeletal vibration of the reduced GO (Nethravathi et al., 2008). The Raman spectra of GO show the D and G bands at 1370 and 1605 cm^{-1}, respectively (Figure 1(b)). The chemical reduction of GO is known to shift these bands to lower wave number and enhances the intensity ratio (I_D/I_G). As expected these bands shifts to 1356 and 1586 cm^{-1} and I_D/I_G value increases to 1.14 from 0.88, indicating the chemical reduction process altered the structures of GO with a plenty of structural defects [Moon et al., 2010]. The significant enhancement in the I_D/I_G ratio of rGO indicates the decrease in the average size of sp^2 domain upon reduction of the exfoliated GO (Zhu et al., 2008; Stankovich et al., 2007). Moreover, in agreement with the earlier literature the Raman spectrum of rGO shows 2D and S3 bands at 2730 and 2943 cm^{-1}, respectively, confirming the better graphitization after reduction (Nethravathi et al., 2008; Wang et al., 2009). The XRD profile of GO shows a peak at $2\theta=10.5$, corresponding to the (002) plane of GO (Figure 1(c)). After reduction this peak completely vanished and a new peak at $2\theta=22.8$ corresponding to (002) plane of rGO was observed, indicating the successful conversion of GO to rGO. The XRD profile of rGO-nPd shows signature for (111), (220), (200), (311) and (222) planes of Pd along with (200) plane of rGO (Figure 1C). The GO and rGO-nPd hybrid material were further characterized with X-ray photoelectron spectroscopic (XPS) measurements (Figure 2). The survey scan spectra of GO shows two peaks at 285.5 and 531.1 eV corresponding to the C 1s and O 1s electrons. On the other hand, survey scan spectra of rGO-nPd shows two new peaks at 335.8 and 341.0 eV along with the C 1s and O 1s electron (Figure S2). The deconvoluted C 1s spectra of GO show three

peaks centered at 284.6, 286.5 and 287.8 corresponding to the C=C/C–C, C–O/C=O and O–C=O functionalities (Lu et al., 2008), respectively (Figure 2(a)). However, a dramatic decrease in the intensity of C 1s peaks at 286.5 and 287.8 eV for the rGO-nPd hybrid material was observed, confirming the removal of oxygen functionalities (Figure 2B). The peaks centered at 335.8 and 341.1 eV in the deconvoluted XPS spectra for Pd (0) are assigned for the Pd $3d_{3/2}$ and Pd $3d_{5/2}$, respectively (Figure 2(b), inset) (Lee et al., 2013).

The transmission electron microscopic (TEM) measurement shows the presence of both nPds and rGO sheets. The nPds have dendritic structure with the branch width of ~50 nm. The magnified image shows that the dendritic nanostructures actually composed of small Pd nanocrystals (Figure 3(a), (b), (c)). GO/rGO in the reaction mixture actually functions as a template and favors the growth of dendritic Pd nanostructure. The high resolution TEM image shows the d-spacing of 0.23 nm (Figure 3(d)), corresponding to the (111) plane of face centered cubic lattice of Pd. The selected area electron diffraction image shows spotty pattern and are indexed to the (111), (220), (200), (311) and (222) planes of Pd (Figure 3(e)). The energy dispersive spectral profile confirms the presence of both Pd and C. The relative atomic percentage of Pd and C was 4.82% and 95.18%, respectively (Figure S3 in the ESM). The electrochemically accessible surface area of the nPd was estimated by cyclic voltammetry in 0.5 M H_2SO_4 solution (Figure S4) according to literature procedure (Rand et al., 1971) and was 2.24 cm^2. The large surface area can be ascribed to the dendritic morphology of the particles and its wide distribution throughout the surface of rGO.

3.3. *Amperometric sensing of H_2O_2*

The function of oxidase-based biosensors involves the quantification of enzymatically generated H_2O_2 during the enzymatic reaction. The amount of H_2O_2 generated is directly proportional to the concentration of the substrate in the sample. In order to evaluate the performance of the transducer based on rGO-nPd in the development of amperometric oxidase-based biosensors, the voltammetric and amperometric response towards H_2O_2 was first examined. Figure 4(a) displays the voltammogram obtained for the oxidation of H_2O_2 on rGO-nPd hybrid material-based transducer. A well-defined voltammetric response for the oxidation of H_2O_2 was obtained at ~0.25 V, which is significantly less positive than the conventional Pt or Pd-based materials (Table S1). The Pt-based materials are known to catalyze the oxidation of H_2O_2 at more positive potential (> 0.4 V) (Karam et al., 2008; Chakraborty et al., 2009). The voltammetric response of rGO-nPd electrode towards H_2O_2 is dependent on the loading of nPd. An observable increase in the peak current and negative shift in the peak potential was noticed while increasing the nanoparticle loading (Figure S5 in the ESM). Highest sensitivity was obtained at the loading of 150 μg/cm^2. Further increment of nanoparticle loading does not increase the sensitivity (Figure S5).

Figure 4(b) shows the amperometric response of rGO-nPd towards H_2O_2. The potential of the electrode was biased at 0.25 V and aliquots of H_2O_2 was injected at regular intervals. Linear increase in the current was observed upon the increasing the concentration of H_2O_2 from 0.1 mM to 17.9 mM and the dynamic range was 0.1 to 33.9 mM (Figure 4(c)). The sensitivity and response time of the electrode was 413.7 ± 0.1 μA/mMcm^2 and 3 s, respectively. Interestingly the electrode could detect H_2O_2 as low as 0.2 nM (S/N=3) (Figure 4(c) inset). The high

sensitivity and low detection limit can be attributed to the large surface area and high catalytic activity of the hybrid material. The high electronic conductivity of rGO nanosheets and the superior catalytic activity of nPds facilitate the electron transfer kinetics for the oxidation of H_2O_2.

The coexisting electroactive bioanalytes such as urate (UA) and ascorbate (AA) are known to interfere the electrochemical detection of H_2O_2 as they generally undergo oxidation almost at the same potential as H_2O_2. In order to examine the interference, amperometric measurement was performed in the presence of the interfering bioanalytes. Interestingly, no amperometric signal was obtained for these analytes implying that they do not interfere the amperometric measurement of H_2O_2 (Figure 4(d)). Moreover, the amperometric signal for H_2O_2 does not change in the presence of large excess of the interfereing analytes (Figure 4(d)). As Nafion® was used as the binder in the preparation of rGO-nPd transducer, it effectively hinder the approach of negatively charged AA and UA by electrostatic repulsion.

3.4. Biosensing of cholesterol ester

The biosensing of cholesterol ester involves the use of bienzymes, cholesterol esterase (ChEt) and cholesterol oxidase (ChOx) and both the enzymes were integrated with the hybrid material for the development of cholesterol biosensor. ChEt hydrolyzes the cholesterol ester and ChOx catalyzes the oxidation of cholesterol in presence of O_2. The enzymatically generated H_2O_2 was detected by the highly sensitive rGO-nPd electrode according to Figure 5(a). Stable amperometric response was obtained for every injection of cholesterol ester (Figure 5(b)); the

amperometric current linearly increases while increasing the concentration of cholesterol ester (5 to 80 μM) (Figure 5(c)). The sensing platform shows the dynamic range from 0.005 to 0.14 mM. The biosensor could detect cholesterol ester as low as 0.05 μM (S/N=3) (Figure S6 in the ESM) and has the response time of 4 s. The sensitivity of the biosensor was 5.12 ± 0.05 μA/μM/cm^2. The high sensitivity and fast response time indicate that the hybrid material and the enzymes are highly accessible to analyte in solution. The apparent Michaelis-Meten constant (K_M^{app}) and the maximum current obtained at saturated level of cholesterol ester (I_{max}) were obtained from Lineweaver-Burk plot and was found to be 1.95 mM and 0.14 mA, respectively. The K_M^{app} value is lower than those of the literature (Yao et al., 1998; Guo et al., 2004; Singh et al., 2004); the lower K_M^{app} value implies strong affinity of substrate to the enzymes presumably due to the hydrophobic nature of the substrate and the surface of the electrode, resulting in a facilitated enzymatic reaction. The biosensing response for cholesterol ester was also performed with the SPE with 50 μL of 0.1 M PBS. Stable and linear response was observed (Figure S7), demonstrating that the hybrid material can be used for the development of disposable biosensor.

3.5. Stability and reproducibility of the biosensor

The biosensor has very good operational and long-term storage stability. No significant change in the amperometric response was observed during continues operation of the biosensor (Figure S8(a)). The long-term storage stability of the biosensor was monitored for 15 days (Figure S8(b)). The biosensor was stored at 4 °C after each measurement. Only 2% decrease after 5 days and 7.2% decrease after 15 days in the initial amperometric current was observed. The reproducibility of the biosensor was evaluated by preparing five individual biosensors in different days at identical condition and the amperometric signal was measured. It was noticed

that the relative standard deviation (RSD) of the amperometric current was only 3% (Figure S9 in the ESM), indicating the excellent reproducibility of the biosensor.

3.6. Real samples analysis

In order to evaluate the performance of the biosensor towards real samples, quantification of total cholesterol in serum and butter was performed. Five individual measurements were performed with each sample and the RSD was calculated from amperometric current. It was found that the RSD values are below 3.5%. In order to validate the results obtained with our biosensor, the quantification of total cholesterol was performed with traditional clinical procedures (Trinder method) (Trinder et al., 1969). It involves the use of the corresponding oxidase-based enzymes and color-indicating reagents. The change in the absorbance was monitored using spectrophotometer. As shown in Table 1, the results obtained with integrated biosensor are in close agreement with clinical results, authenticating the reliability of the proposed nPd-rGO-based biosensor.

4. Conclusions

We have demonstrated a new protocol for the synthesis of hybrid material based on Pd nanoparticles and rGO. Facile reduction of GO was achieved using Zn and Pd precursor. The in situ generated nPd essentially increase the local concentration of nascent hydrogen. The in situ generated atomic hydrogen and hydrogen intercalated nPd efficiently reduces GO to rGO. The as-synthesized rGO-nPd material has high electrocatalytic activity towards oxidation of H_2O_2 at the potential of 0.25 V, which is significantly lower than those of the existing electrocatalyst. The hybrid material-based platform is highly sensitive and it could detect H_2O_2 at sub-nanomolar

level without any mediator or enzyme. The biosensor has high sensitivity, stability and it does not suffer from the interference due to easily oxidizable electroactive analyte. The oxidase based cholesterol biosensor was developed using enzymes ChOx and ChEt. The rGO-nPd biosensor shows high sensitivity and very fast response time. The stability and reproducibility of the biosensor is outstanding. Practical application of the biosensor is demonstrated by the analysis of total cholesterol in human serum samples and butter. The rGO-nPd hybrid material is very promising for the development of biosensing platforms. It is worth to point out here that the rGO-nPd hybrid material can also be used in the development of oxidase-based amperometric first generation biosensors for other metabolites such as lactate, glutamate, glucose, uric acid, etc.

Acknowledgements

R. S. Dey is recipient of UGC research fellowship. This work was financially supported by DST and CSIR, New Delhi. Authors are thankful to B. C. Roy Technology Hospital, IIT Kharagpur for human serum samples and the clinical laboratory analysis of cholesterol. We acknowledge DST-FIST for X-ray diffractometer facility.

Appendix. Supporting Information

Supporting information associated with this article can be found in the online version at http://dx.doi.org/**********).

References

Artiles, M. S., Rout, C. S., Fisher, T. S. 2011. Adv. Drug Delivery Rev. 63, 1352–1360.

Barman, B. K., Nanda, K. K. 2013. Chem. Commun, 49, 8949-8951.

Chakraborty, S., Raj, C. R. 2009. Biosens. Bioelectron. 24, 3264–3268.

Cheng, I. F., Fernando, Q., Korte, N. 1997. Environ. Sci. Technol. 31, 1074–1078.

Cui, S., Mao, S., Lu, G., Chen, J. 2013. J. Phys. Chem. Lett. 4, 2441-2454.

Dey, R. S., Hajra, S., Sahu, R. K., Raj, C. R., Panigrahi, M. K. 2012. Chem. Commun., 48, 1787-1789.

Dröge, W., Schipper, H. M. 2007. Aging Cell, 6, 361-370.

Fang, Y., Guo, S., Zhu, C., Zhai, Y., Wang, E. 2010. Langmuir, 26, 11277–11282.

Guo, M., Chen, J., Li, J., Nie, L., Yao, S. 2004. Electroanalysis, 16, 1992–1998.

Guo, S., Dong, S., Wang, E. 2010. ACS Nano, 4, 547-555.

Gutés, A., Carraro, C., Maboudian, R. 2012. Biosens. Bioelectron. 33, 56–59.

He, F-A., Fan, J.-T., Song, F., Zhang, L.-M., Chan, H. L.-W. 2011. Nanoscale, 3, 1182-1188.

Hrapovic, S., Liu, Y., Male, K. B., Luong, J. H. T. 2004. Anal. Chem. 76, 1083–1088.

Hummers, W., Offeman, R. 1958. J. Am. Chem. Soc. 80, 1339–1339.

Jin, Z., Nackashi, D., Lu, W., Kittrell, C., Tour, J. M. 2010. Chem. Mater., 22, 5695–5699.

Karam, P., Halaoui, L. I. 2008. Anal. Chem. 80, 5441–5448.

Kovtyukhova, N. I., Ollivier, P. J., Martin, B. R., Mallouk, T. E., Chizhik, S. A., Buzaneva, E. V., Gorchinskiy, A. D. 1999. Chem. Mater. 11, 771– 778.

Lee, K. H., Han, S.-W., Kwon, K.-Y., Park, J. B. 2013. J. Colloid Interface Sci., 403, 127–133.

Li, C., Hu, J., Liu, T., Liu, S. 2011. Macromolecules, 44, 429-431.

Lightcap, I. V., Kamat, P. V. 2013. Acc. Chem. Res., 46, 2235–2243.

Lu, J., Do, I., Drzal, L. T., Worden, R. M., Lee, I. 2008. ACS Nano 2, 1825–1832.

Moon, I. K., Lee, J., Ruoff, R. S., Lee, H. 2010. Nat. Comm. 1, 73-78.

Motonaka, J., Faulkner, L. R. 1993. Anal. Chem. 65, 3258–3261.

Myant, N. B. in The biology of cholesterol and related steroids, William Heinemann Medical Books: London, 1981.

Nethravathi, C., Rajamathi, M. 2008. Carbon, 46, 1994-1998.

Peña, N., Ruiz, G., Reviejo, A. J., Pingarrón, J. M. 2001. Anal. Chem. 73, 1190-1195.

Prashant V. Kamat, 2010. J. Phys. Chem. Lett. 1, 520–527.

Pumera, M. 2011. Mat. Today, 14, 308-315.

Raj, C. R. Towards biosensing with graphene-based materials, in Innovative graphene technologies: Evaluation and application, volume 2, chapter 10, Rapra Smithers, UK, 2013.

Rand, D. A. J., Woods, R. 1971. J. Electroanal. Chem. 31, 29-38.

Rhee, S. G. H_2O_2, 2006. Science, 312, 1882-1883.

Safavi, A., Maleki, N., Tajabadi, F., Farjami, E. 2007. Electrochem. Commun. 9, 1963-1968.

Sevanian, A., Hochstein, P. 1985. Annu. Rev. Nutr. 5, 365-390.

Singh, S., Chaubey, A., Malhotra, B. D. 2004. Anal. Chim. Acta 502, 229–234.

Stankovich, S., Dikin, D. A., Piner, R. D., Kohlhaas, K. A., Kleinhammes, A., Jia, Y., Wu, Y., Nguyen, S. T., Ruoff, R. S. 2007. Carbon, 45, 1558–1565.

Tian, J., Deng, S.-Y., Li, D.-L., Shan, D., He, W., Zhang, X.-J., Shi, Y. 2013. Biosens. Bioelectron. 49, 466–471.

Trinder, P. 1969. Ann. Clin. Biochem. 6, 24−25.

Wang, H., Robinson, J. T., Li, X., Dai, H. 2009. J. Am. Chem. Soc. 131, 9910–9911.

Wang, Y., Chang, H., Wu, H., Liu, H. 2013. J. Mater. Chem. B. 1, 3521-3534.

Weast, R. C., Astle, M. J., Beyer, W. H. Handbook of Physics and Chemistry, 64th ed., CRC Press, Boca Raton (1983-1984).

Xu, Y. X., Bai, H., Lu, G. W., Li, C., Shi, G. Q. 2008. J. Am. Chem. Soc. 130, 5856–5857.

Yang, J., Tian, C., Wang, L., Fu, H. 2011. J. Mater. Chem., 21, 3384-3390.

Yang, M., Yang, Y., Liu, Y., Shen, G., Yu, R. 2006. Biosens. Bioelectron. 21, 1125–1131.

Yao, T., Takashima, K. 1998. Biosens. Bioelectron. 13, 67–73.

Zan, X., Fang, Z., Wu, J., Xiao, F., Huo, F., Duan, H. 2013. Biosensor. Bioelectron. 49, 71-78.

Zhu, Y. W., Murli, S., Cai, W. W., Li, X. S., Suk, J. W., Potts, J. R., Ruoff, R. S2010. Adv. Mater. 22, 3906-3924.

Highlights

- New method for the synthesis of rGO-Pd nanoparticle functional hybrid is developed.
- Amperometric sensing of hydrogen peroxide with detection limit of 0.2 nM is achieved.
- Biosensing of total cholesterol is demonstrated at 0.25 V without any interference.
- Total cholesterol in human serum is quantified.

Figures, Scheme and Table

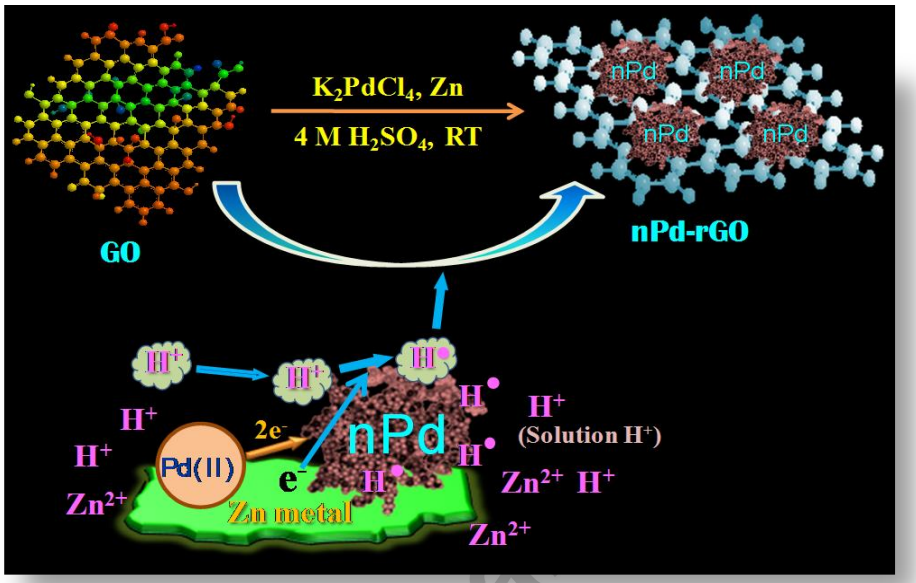

Scheme 1

Scheme illustrating the possible mechanism involved in the synthesis of rGO-nPd hybrid material.

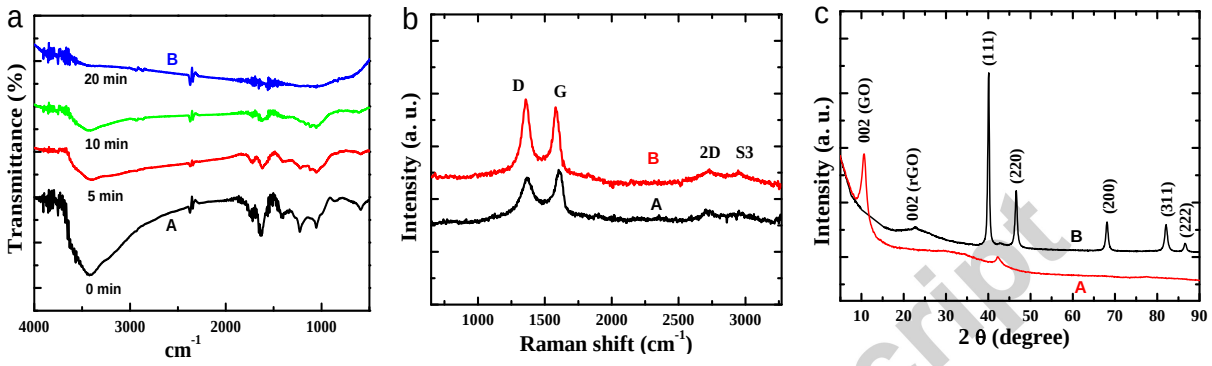

Figure 1

Time-dependent FTIR (a) and Raman spectra (b) and XRD profile (c) obtained for GO (A) and rGO-nPd (B).

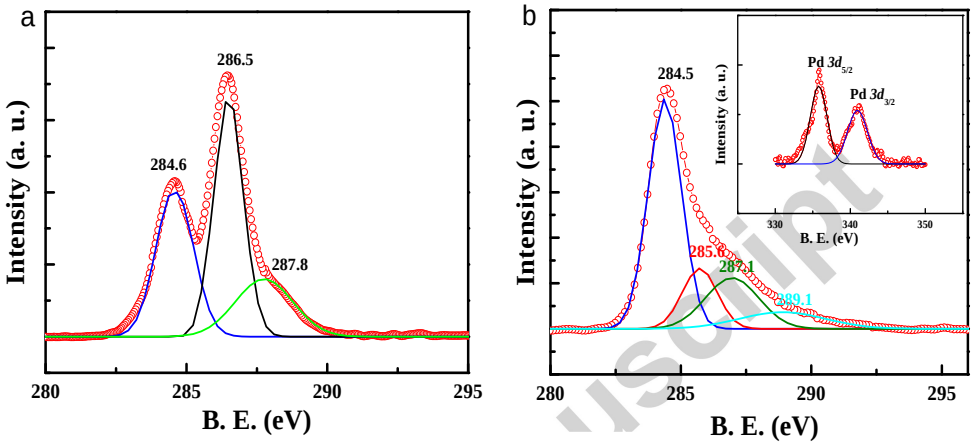

Figure 2

C 1s XPS profile of GO (a) and rGO-nPd (b). Inset in (b) is the 3d signal of Pd.

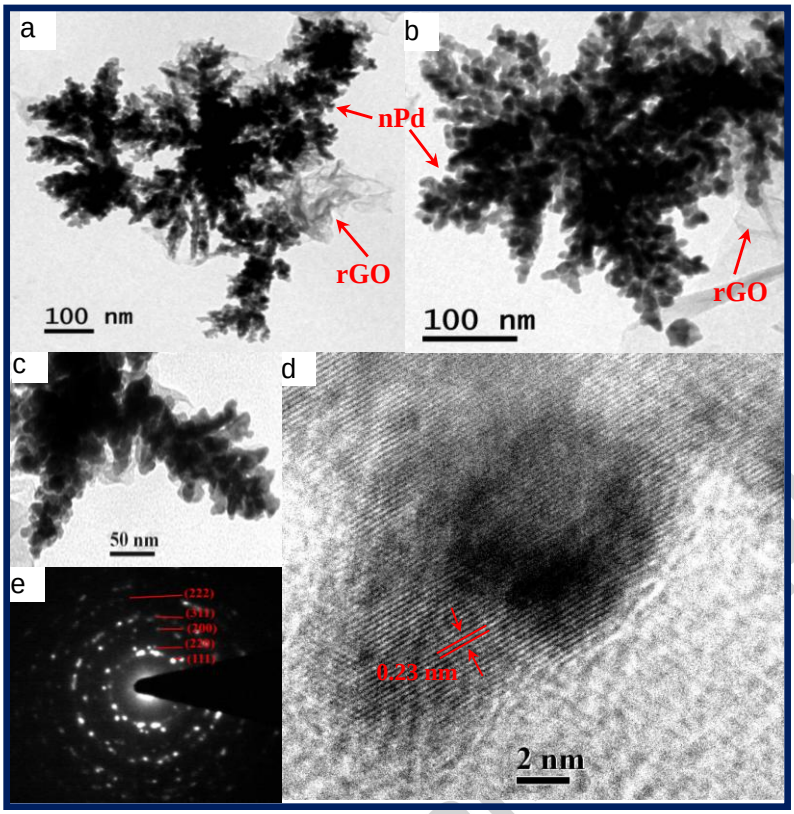

Figure 3

TEM (a,b,c) and HRTEM (d) images and SAED pattern (e) of rGO-nPd.

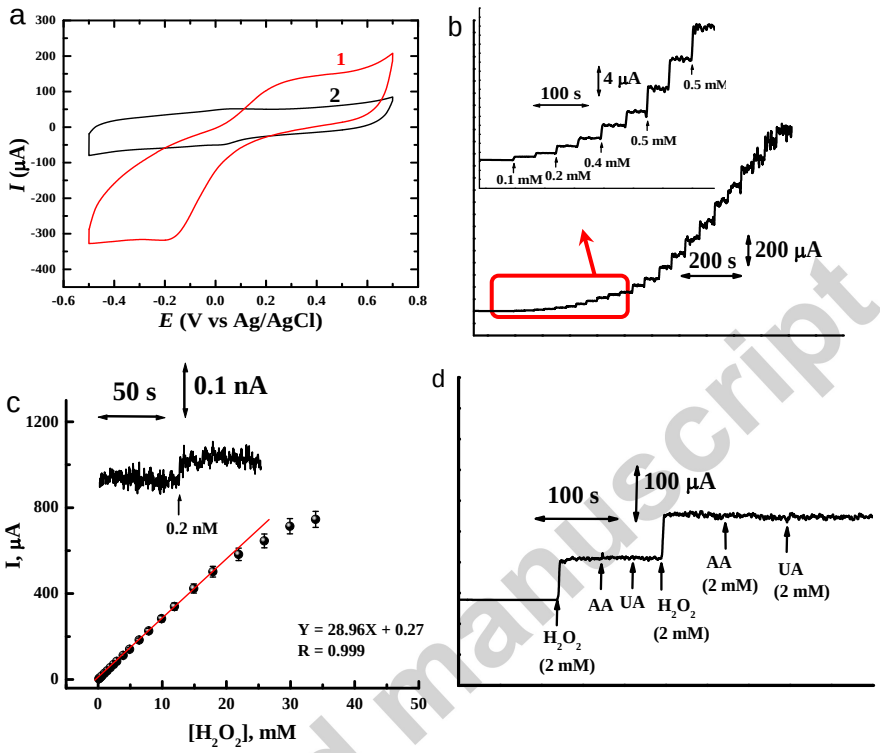

Figure 4

Cyclic voltammetric (a) response of rGO-nPd electrode in the absence (1) and in presence (2) of H_2O_2 (2 mM) in PBS. Amperometric (b) response of rGO-nPd electrode towards H_2O_2. Aliquot of H_2O_2 was injected into the stirred supporting electrolyte (PBS, pH 7.2). Potential of the electrode was held at 0.25 V. Inset is the magnified version as indicated by arrow. Corresponding calibration plot is shown in (c). Inset in (c) is the amperometric response of the electrode for 0.2 nM H_2O_2. Amperometric (d) response illustrating the interference free sensing of H_2O_2. Ascorbate, H_2O_2, and urate (2 mM each) were injected at regular interval as indicated. rGO-nPd loading: 150 μg/cm^2.

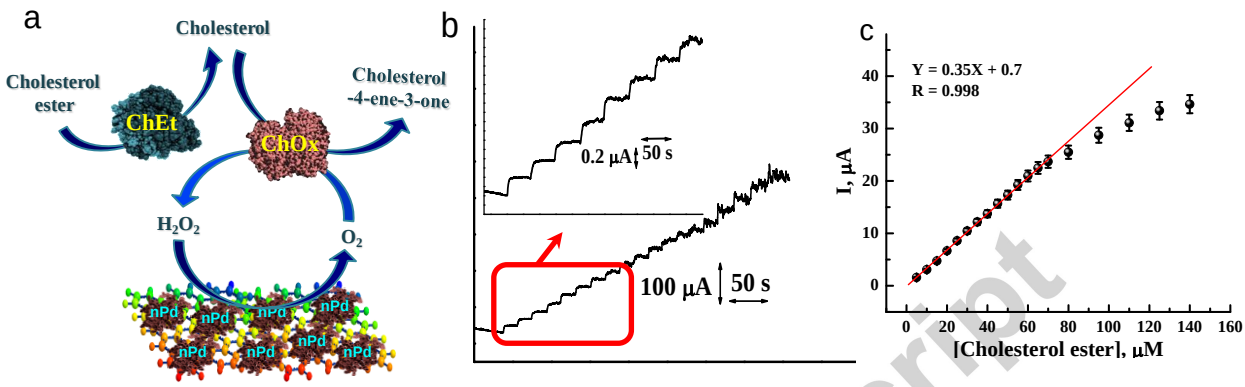

Figure 5

Figure (a) illustrating the biosensing of cholesterol ester with enzyme integrated rGO-nPd-based biosensor. Amperometric (b) response obtained for the sensing of cholesterol ester. Corresponding calibration plot is shown in (c). Other experimental conditions are same as in Figure 4.

Table 1 Biosensing of cholesterol (total) in human serum and butter samples.

Sample	Sample No.	Measured with rGO-nPd biosensor* (mg/dL)	Measured by clinical method (mg/dL) or Commercial value[§]	RSD (%)
Serum	1	130.0	130	3.45
	2	111.6	122	1.51
Butter	1	0.175[§]	0.18[§]	2.62

RSD: obtained from five individual measurements of each samples

* Average of five independent measurements

[§] g/100g